Journal of Agriculture and Food Research 14 (2023) 100875

Contents lists available at ScienceDirect

Journal of Agriculture and Food Research

journal homepage: www.sciencedirect.com/journal/journal-of-agriculture-and-food-research

Modeling the daily dynamics of grass growth of several species according to their functional type, based on soil water and nitrogen dynamics: Gras-Sim model definition, parametrization and evaluation

Essomandan Urbain Kokah [a,b,*], David Knoden [c], Richard Lambert [c,d], Hamza Himdi [d], Benjamin Dumont [a,1], Jérôme Bindelle [a,b,1]

[a] TERRA – AgricultureIsLife/EnvironmentIsLife, Gembloux Agro-Bio Tech, University of Liege, Passage des Déportés 2, 5030 Gembloux, Belgium
[b] AgroBioChem, Precision Livestock and Nutrition, Gembloux Agro-Bio Tech, University of Liege, Passage des Déportés 2, 5030 Gembloux, Belgium
[c] Fourrages Mieux ASBL, Horritine 1, 6600 Bastogne, Belgium
[d] Earth and Life Institute, Catholic University of Louvain, Croix du sud 2, 1348 Louvain La Neuve, Belgium

ARTICLE INFO

Keywords:
Model
Functional group
Grassland
Biomass
Nitrogen
Water

ABSTRACT

Gras-Sim model, through the environmental conditions and the dynamics of water and nitrogen in the soil, enables the prediction of the biomass yield in permanent grasslands. It was developed from existing models and simulates the dynamics of several grass species grouped into plant functional types (PFTs) A and B. Model inputs include weather data, fertilizer application, soil data, and cutting management. In contrast to previous models, Gras-Sim proposes a complete nitrogen balance at the field scale as well as a new formalism to estimate actual evapotranspiration based on the crop coefficient (Kc) for a better prediction of biomass production even under moderate stress. Gras-Sim was evaluated in this paper on the basis of data from experiments conducted between 2010 and 2018, on 3 sites fairly representative of the soil and climate conditions in Wallonia (Belgium). The relative root mean square error (RRMSE), normalized deviation (ND), and model efficiency (EF) across all cuts, sites, and PFTs were 29 %, 2 %, and 71 % respectively, for biomass production. Gras-Sim is a simple and efficient model that can be used as a starting point for the design of a decision support tool for better management of permanent grasslands.

1. Introduction

Grasslands provide many ecosystem services to mankind. They are of environmental, cultural and economic interest. Herbage from grasslands, whether they are permanent or temporary, grazed or cut, mono or multi-species, remains the cheapest and highest quality food source for herbivores in temperate zones [1,2] providing them with an important source of energy [3].

Permanent grasslands can present a wide diversity and richness in species which will respond differently to weather conditions, management practices [4], and soil physico-chemical properties [5,6]. For a given plant community, the list of species present can be very long, which sometimes makes it difficult to diagnose the agricultural (productivity, nutritional value, flexibility, and precocity) and environmental (species diversity) use value of the grassland [7], while such a diagnostic is a prerequisite for a better management. To overcome this difficulty, Cruz et al. [7] suggested to regroup the different plants species present on a given grassland according to some key functional traits. Functional traits are morphological, biochemical, physiological, structural, phenological, or behavioral characteristics that are expressed in phenotypes of individual organisms and are considered relevant to the response of such organisms to the environment or their effects on ecosystem properties [8]. Particularly, in terms of grassland diagnostics and decision-making, it allows to replace the long list of species in the plant community by a series of plant functional types (PFTs) to which the dominant species belong. The first classification for permanent temperate grasslands was later extended to additional functional types and adapted to other pedoclimatic contexts [9,

* Corresponding author. TERRA – AgricultureIsLife/EnvironmentIsLife, Gembloux Agro-Bio Tech, University of Liege, Passage des Déportés 2, 5030 Gembloux, Belgium.
E-mail address: eukokah@uliege.be (E.U. Kokah).
[1] Authors share senior co-authorship.

https://doi.org/10.1016/j.jafr.2023.100875
Received 21 August 2023; Received in revised form 12 October 2023; Accepted 11 November 2023
Available online 17 November 2023

10]. This classification focused on 17 grass species and grouped them in four PFTs, namely types A, B, C, and D. Plants were divided into these PFTs according to their ability to capture and preserve resources, their response to fertility, and the speediness of organs recycling. PFT A regroups species displaying and early development at the beginning of the growing season with high growth rates but not allowing a high accumulation of standing biomass (e.g.*Lolium perenne*); PFT B regroups slightly later species allowing a high accumulation of standing biomass (e.g. *Dactylis glomerata*); PFT C holds slower growing species of lesser quality (e.g. *Festuca rubra*); and PFT D, species with late phenology and low nutritional value (e.g. *Briza media*). This classification was later extended from 4 to 6 PFTs to better classify 38 temperate grass species [10]. The two additional PFTs regrouped on the one hand, species with characteristics in between those of PFTs B and C (e.g. *Trisetum flavescens*), and, on the other hand, annual grasses.

Since grasslands are quite complex ecosystems and future weather conditions are difficult to reproduce under experimental conditions, it is difficult to explore in vivo how grassland management strategies will adapt to future climatic conditions. Moreover, farmers work in an ever-changing environment due in particular to weather variability. Hence, decision-making by farmers could be greatly improved if they could project the impact of their operational choices on their grasslands. Modeling work has already been done in this direction, using climate scenarios to predict the effects of management on grasslands productivity and organic carbon sequestration [11–14]. For the future climate, these models used site-specific data from the RCP (Representative Climate Pathways) scenarios provided by the Intergovernmental Panel on Climate Change (IPCC).

Mathematical mechanistic vegetation models allow the study of long and short-term plant dynamics in the face of weather variability and management strategies. Several models already address the grass growth dynamics. Most of them simulate monospecific or species-dominated grasslands, in particular that of the perennial ryegrass (*Lolium perenne*), under cutting conditions [15–17] or grazing by taking into account the impact of the grazing process on the sward [18–21].

Given the high specific diversity of grasslands, it is not possible for a model to consider all species. Some models, such as ModVege [22,23] and DynaGraM [24,25], simulate grassland dynamics not as a set of species, but as a set of PFTs. ModVege is a mechanistic and deterministic model that simulates the daily dynamics of biomass production, structure and digestibility in permanent grasslands. Criticisms of this model are mainly related to the lack of a soil compartment and its tendency to overestimate the impact of moderate water stress on production [26].

An extension of ModVege was proposed by Ruelle et al. [20] in the Moorepark St Gilles grass growth model (MoSt GG) by integrating soil nitrogen dynamics. However, MoSt GG remains limited to a single functional type, namely PFT A, as it has been validated for *Lolium perenne*. The aim of this study is to complement this previous work by developing a model capable of simulating the response of a large number of grassland species to different management strategies at field scale based not only on climatic conditions, but also on soil and plant nitrogen dynamics. Therefore, a "soil" compartment based on CATIMO model [27] was developed to close the water and nitrogen balance in the soil and plant at the grassland scale. In addition to PFT A, Gras-Sim was parameterized to simulate the dynamics of PFT B species. The model also proposes a new formalism for estimating the actual evapotranspiration from potential evapotranspiration based on the work of Liu et al. [28] to allow good predictive performances even under moderate water stress conditions. Gras-Sim can be used to simulate whole-farm production, as its outputs can be used directly as inputs to a ruminant intake model. The work involved (i) developing the model entirely in R Studio, (ii) setting parameter values based on literature, field data, and simulations, (iii) evaluating the model by comparing simulation results with field data, and (iv) performing sensitivity analysis on some key model parameters. This paper presents the formalism of the model and the results of its validation under Walloon conditions in Belgium.

2. Materials and methods

Gras-Sim is a mechanistic model that simulates the daily dynamics of biomass production in managed grasslands. Its core is based on ModVege designed to be interoperable with the animal component, although this was not considered in the present work. Conceptually, Gras-Sim is based on a functional approach rather than a species-based approach to account for the diversity of plant species. In other words, a grassland is nothing more than the sum of the average biological properties (functional traits) of its plant community. Interspecific competition for resources and other interactions that may exist in a multi-species grassland are not considered.

2.1. Model structure

As in ModVege, Gras-Sim simulates the dynamics of biomass divided into four compartments (Fig. 1) that represent the structural components of the grass. These are vegetative biomass (leaves and sheath) green (GV) and dead (DV), and reproductive biomass (stems and flowers) green (GR) and dead (DR). Each compartment is characterized by its biomass (BM), its age (AGE), and the digestibility of its organic matter (OMD). The model simulates the daily dynamics of the grassland as a combination of the changes within and the fluxes between these four compartments. The biomass growth, senescence, and abscission are described as continuous fluxes. To keep the model relatively simple and practical, with input data easily measured in the field, only aboveground biomass is simulated, as in the previous CATIMO, ModVege, and MoSt GG models. In Gras-Sim, soil and plant water and nitrogen dynamics were adapted mainly from CATIMO model as detailed later.

Hence, the model works on the basis of 17 state variables that can be grouped into two categories: those related to the state of the biomass ant its N content and those related to the dynamics of water and nitrogen in the soil (Table 1). These state variables evolve under the influence of the input variables. The latter can also be grouped into two categories: environmental variables and management variables (Table 1).

2.2. Biomass dynamics

Biomass accumulation is influenced by environmental conditions and soil water and nitrogen dynamics (Fig. 1). The flow diagram of biomass dynamics submodel for PFTs A and B is shown in Appendix B (Fig. B1). Daily plant growth (*GRO*, kg DM ha^{-1}) is driven by potential growth (PGRO) obtained under optimum conditions and limited by both environmental factors (*ENV*) and seasonal effect (*SEA*) of the shoot growth (Eq. (1)), conditioned by the storage and mobilization of reserves [22]:

$$GRO = PGRO \times ENV \times SEA \quad (1)$$

PGRO (kg DM ha^{-1}) varies according to the incident photosynthetically active radiation (MJ m^{-2}), the maximum efficiency of use of this radiation by the plant (g DM MJ^{-1}), and the leaf area index. The full equation is given in appendix A (Eq. (A.1)). *SEA* varies according to the functional group ranging from 0.5 to 1.5 for the PFTs A and B considered in this study. The formalism of *SEA* is also presented in appendix A (Eq. (A.3)). *SEA* values below 1 indicate that the plant is building up underground reserves. They are higher than 1 when the plant is using its energy reserves. ENV holds environmental limitations to the potential growth, ranging between 0, no growth, and 1, no limitation to the growth. It combines four functions (Eq. (2)), related to plant nitrogen nutrition status (*fN*), adapted from the CATIMO model, temperature *fT*, photosynthetically active radiation (*fPARi*), and soil water (*fW*). All these functions vary between 0 and 1 (Eqs. (A.12), (A.13), (A.14), (A.17), (A.18), (A.19)):

$$ENV = fPARi \times fN \times \min(fT, fW) \quad (2)$$

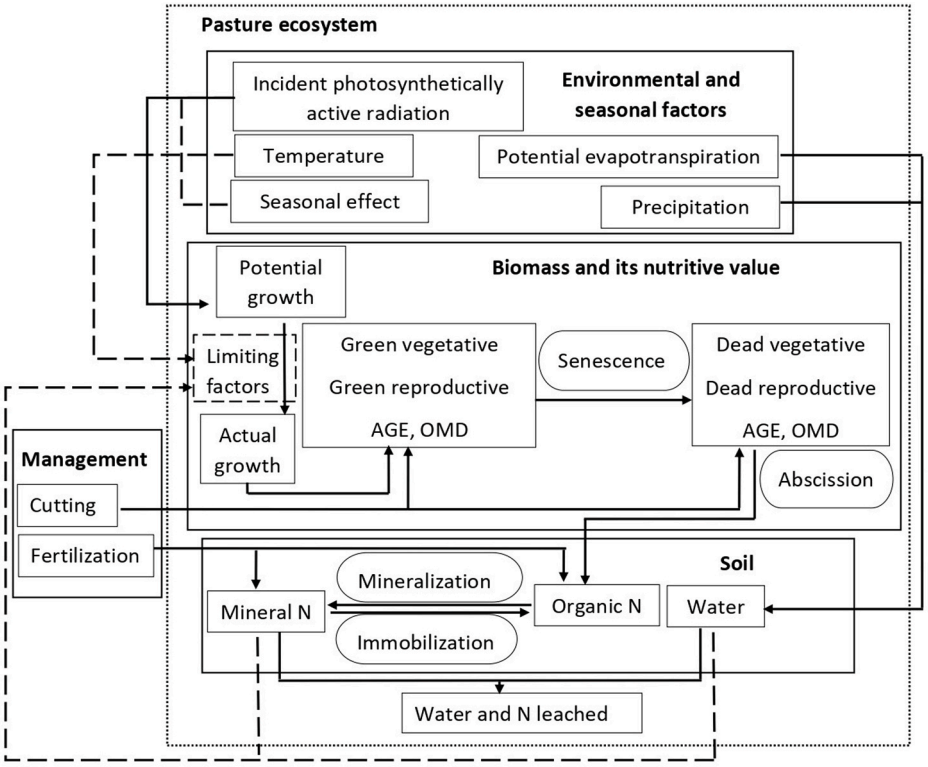

Fig. 1. Structure of the Gras-Sim model. Rectangular boxes represent state variables (biomass, mineral and organic N pools, and soil water) and driving variables (management, climate, and seasonal effects). Processes are represented by the rounded boxes on the sides. Solid arrows show direct and feedback effects of different variables, and dotted arrows show limiting effects on growth.

2.3. Soil water and actual evapotranspiration

The water stress function (*fW*, Eq. (2)), which influences the daily growth of the plant, is the ratio between soil water (Eq. (4)) and water holding capacity. This factor is therefore 1 (no stress) when the soil water content is at field capacity:

$$WaterCapacity = \begin{pmatrix} 0.2576 - 0.002 \times Sand + 0.0036 \times Clay + \\ 0.0299 \times OM \end{pmatrix} \times 1000 \quad (3)$$

where *Sand*, *Clay*, and *OM* stand respectively for the proportion (%) of sand, clay, and organic matter in the soil. On a given day the soil water (*Water*, mm) balance is calculated as the sum of the rainfall (*PP*, mm) and the surplus of water from the previous day(*notRunoff*, mm), if any, from which the water lost by evapotranspiration (*AET*, mm) and leaching (*WaterLeached*, mm) is removed:

$$\frac{dWater}{dt} = PP + notRunoff - AET - WaterLeached \quad (4)$$

The equations to calculate *notRunoff* and *WaterLeached* are presented in Appendix A (Eqs. (A.44), (A.45)). If the soil water content is above the saturation point (*WaterSaturation*, mm (Eq. (A.42)), 20 % of the surplus water (*notRunoff*) is kept on the plot and is be added to the water reserve of the next day [20]. To avoid overestimating the impact of heat stress on growth, especially in periods of moderate stress as was the case with ModVege, Gras-Sim proposes a new formalism for estimating actual evapotranspiration (*AET*, Eq. (5)). This formalism is widely used in water management under crops but very little used for grasslands:

$$AET = Kc \times PET \quad (5)$$

where *PET* (mm) denotes the potential evapotranspiration measured in the field and Kc is crop coefficient whose monthly average value for grassland is given by Liu et al. [28]. Kc is the crop coefficient from crop models. Kc varies according to several factors including species, canopy conductance, leaf area index, height, and soil characteristics. Kc values for grasslands used in Gras-Sim, given in appendix B (Table B2), are based on the measurements made over 8 years (2000–2007) on the different sites of the FLUXNET network including those in France,

Table 1
Variables used in Gras-Sim model.

Variables	Symbol	Unit
Biomass variables		
Standing green vegetative biomass	BMGV	kg DM ha^{-1}
Standing green reproductive biomass	BMGR	kg DM ha^{-1}
Standing dead vegetative biomass	BMDV	kg DM ha^{-1}
Standing dead reproductive biomass	BMDR	kg DM ha^{-1}
Mean age of biomass in GV compartment	AGEGV	°C. d
Mean age of biomass in GR compartment	AGEGR	°C. d
Mean age of biomass in DV compartment	AGEDV	°C. d
Mean age of biomass in DR compartment	AGEDR	°C. d
Organic matter digestibility of BMGV	OMDGV	g g^{-1}
Organic matter digestibility of BMGR	OMDGR	g g^{-1}
Green vegetative biomass N content	NQGV	kg N ha^{-1}
Green reproductive biomass N content	NQGR	kg N ha^{-1}
Dead vegetative biomass N content	NQDV	kg N ha^{-1}
Dead reproductive biomass N content	NQDR	kg N ha^{-1}
Soil variables		
Soil water content	Water	mm
Soil organic nitrogen	Norg	kg N ha^{-1}
Soil mineral nitrogen	Nmin	kg N ha^{-1}
Environmental variables		
Mean daily temperature	Temp	°C
Incident photosynthetically active radiation	PARi	MJ m^{-2}
Actual evapotranspiration	AET	mm
Rainfall	PP	mm
Management variables		
Total quantity of mineral N applied	NminFerti	kg N ha^{-1}
Total quantity of organic N applied	NorgFerti	kg N ha^{-1}
Proportion of mineral N if organic	PropNmin	–

Table 2
Number of cuts performed over the entire period for all varieties, sites, and plant functional types (PFTs). Michamps (MCP), Louvain-la-Neuve (LLN), and Tinlot (TLT).

Year	Site	PFT	Cuts
2010	MCP	A	3
2011	MCP	A	4
2012	MCP	A	3
2013	LLN	B	4
2014	LLN, MCP, TLT	B	15
2015	LLN, MCP, TLT	B	10
2016	LLN, MCP, TLT	A, B	15
2017	LLN, MCP, TLT	A	7
2018	LLN, TLT	A	5

Belgium, and Germany [28]. In Gras-Sim, the water at wilting point and field capacity is calculated according to the equations of MoSt GG model. These different equations are presented in appendix A (Eqs. (A.40), (A.41)).

2.4. Organic matter digestibility

The organic matter digestibility in green vegetative (*OMDGV*, g g^{-1}) and reproductive (*OMDGR*, g g^{-1}) compartments evolves with the age of the plant. The maximum digestibility (*maxOMDGV*, *maxOMDGR*, g g^{-1}), a theoretical value at zero age, will progressively decrease to reach its minimum (*minOMDGV*, *minOMDGR*, g g^{-1}) value at the maximum age, which is the leaf life span (*LLS*, °C d) for the green vegetative (GV) compartment and the duration of the reproductive period ($ST2 - ST1$, °C d) for the green reproductive (GR) compartment [22]:

$$OMDGV = maxOMDGV - AGEGV \times \frac{(maxOMDGV - minOMDGV)}{LLS} \quad (6)$$

$$OMDGR = maxOMDGR - AGEGR \times \frac{(maxOMDGR - minOMDGR)}{(ST2 - ST1)} \quad (7)$$

where *AGEGV* (°C d) denotes the age of the biomass in the GV compartment and *AGEGR* (°C d), the age of the biomass in the GR compartment. The daily dynamics of the age of green and dead vegetation is presented in appendix A (Eqs. (A.25), (A.26)). The values of the parameters *maxOMDGV*, *maxOMDGR*, *minOMDGV*, *minOMDGR*, *ST*1, and *ST*2 are presented in appendix B (Table B1). As assumed in ModVege, the digestibility of the dead plant compartments (*OMDDV*, *OMDDR*) is constant (Table B1).

2.5. N dynamics in soil and plant

The dynamics of N in the soil is essentially based on the CATIMO and MoSt GG models. GASSQUAL provides a N balance at the grassland scale. The flow diagram of the soil water and nitrogen dynamics submodel is shown in Appendix B (Fig. B2).

2.5.1. Soil N supply

The nitrogen supply (*Nsupply*, kg N ha^{-1}) from the soil to the plant depends not only on the available mineral N (*Nmin*, kg N ha^{-1}) but also on other factors such as the capacity of the root system to absorb it (Eq. (8)). As the below-ground biomass is not considered in Gras-Sim, a *Nmin* availability factor (*FNA*) is define as described by Bonesmo and Bélanger [27].

$$Nsupply = Nmin \times FNA \quad (8)$$

where

$$FNA = \min\left(FNA_{max}, FNA_{max} \times \frac{Nmin}{NS_C}\right) \quad (9)$$

Beyond NS_C (kg N ha^{-1}), a critical threshold of *Nmin*, *FNA* is assumed to be constant. This threshold corresponds to the *Nmin* content for maximum availability. Its value is given in Appendix B (Table B3). FNA_{max} is the maximum absorbable fraction of available *Nmin* (Table B3).

2.5.2. N status in the plant

The state of nitrogen nutrition, designated in Gras-Sim by the relative

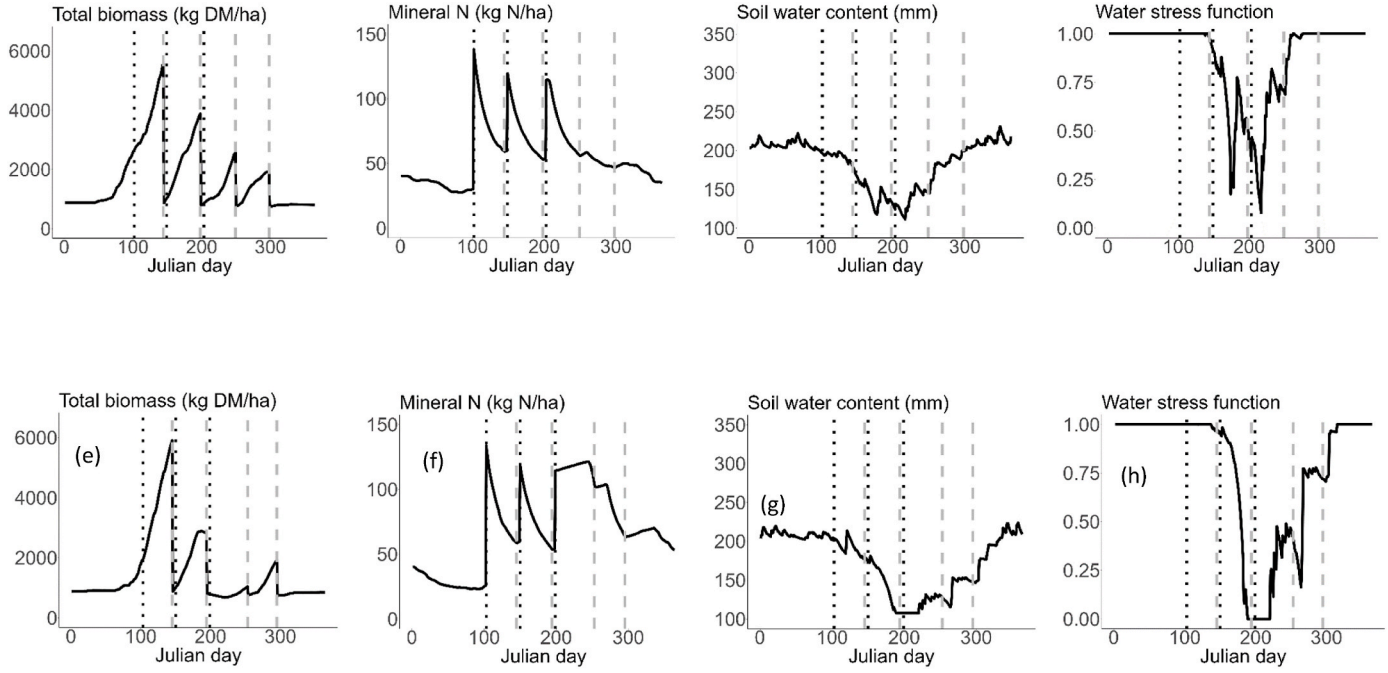

Fig. 2. Dynamics of above-ground biomass, soil water and nitrogen, and water stress function, simulated by Gras-Sim on the Louvain-la-Neuve (LLN) site for PFT A over two consecutive years: 2017 ((a), (b), (c), and (d)) and 2018 ((e), (f), (g), and (h)). The grey dashed lines correspond to cutting dates and the black dashed lines correspond to fertilization dates.

Table 3
Weather data collected during the trial years on The Michamps (MCP), Louvain-la-Neuve (LLN), and Tinlot (TLT) sites. T (temperature), Ra (radiation), PP (precipitation), and PET (potential evapotranspiration). The values between brackets are standard deviation.

	T (°C)	Ra (MJ m^{-2} d^{-1})	PP (mm)	PET (mm)
MCP				
2010	6.89 (7.62)	11.64 (9.09)	829	572
2011	8.8 (6.03)	10.91(8.09)	777	338
2012	7.92 (6.8)	10.26(7.68)	1105	422
2014	9.38 (5.59)	10.54 (8.28)	731	556
2015	8.97 (6.5)	10.31 (8.09)	756	547
2016	8.54 (6.75)	10.18 (7.52)	699	521
2017	8.81 (6.86)	10.71 (8.03)	798	578
LLN				
2013	10.16 (6.96)	11.15 (8.39)	608	665
2014	11.6 (5.38)	10.26 (7.14)	692	689
2015	10.83 (5.91)	10.82 (8.58)	640	725
2016	10.49 (6.51)	10.46 (7.21)	667	664
2017	10.92 (6.58)	10.37 (7.6)	605	724
2018	11.59 (7.35)	11.26 (8.11)	499	815
TLT				
2014	11.87 (5.61)	10.38 (7.69)	808	661
2015	11.28 (6.32)	11.42 (8.69)	668	684
2016	10.64 (6.9)	10.88 (7.59)	712	637
2017	10.03 (6.75)	10.61 (7.93)	677	661
2018	10.9 (7.46)	11.53 (8.33)	600	755

N concentration (*RNC*) is an important factor influencing the growth of the plant. It is the ratio between the actual N concentration *Nact* (g N 100 g^{-1} DM) to the critical N concentration (*Ncrit*):

$$RNC = \frac{Nact}{Ncrit} \tag{10}$$

Ncrit (%) is calculated on the basis of the exportable biomass, i.e. the biomass above 5 cm (*BMover*5, kg DM ha^{-1}). It is the same for the PFTs A and B. *Ncrit* follows the critical N dilution curve described by Lemaire et al. [29]:

$$Ncrit = \min\left(4.8, 4.8 \times (BMover5)^{-0.32}\right) \tag{11}$$

The *Nact* calculation is also based on exportable biomass (Eq. (A.7)).

2.5.3. Plant N demand and actual uptake

The daily N demand of the plant (*Ndemand*, kg N ha^{-1}) is the difference between the amount of N needed to increase the actual N content of the plant (*Nact*) under limited conditions to the maximum limit of N absorption (*Nmax*,(%)) [27]:

$$Ndemand = \frac{(BMGV + BMGR) \times (Nmax - Nact)}{FNH} \tag{12}$$

Nmax (Eq. (13)) follows the N dilution curve of the aboveground biomass and varies with plant functional type (PFT) [30,31]. *BMGV* and *BMGR* (kg DM ha^{-1}) correspond to the biomass of the green compartments (Eq. (A.31)).

$$Nmax = \min\left(\alpha_{max}, \alpha_{max} \times (BMover5)^{-\beta_{max}}\right) \tag{13}$$

The values of the parameters α_{max} (%) and β_{max} (dimensionless) are given in appendix B (Table B3) according to the PFT. *BMover*5 (t DM ha^{-1}) represents the total exportable biomass (above 5 cm of grass height). The nitrogen actually absorbed by the plant is the minimum between the mineral N supply of the soil and the N demand to meet its needs:

$$Nuptake = \min(Nsupply, Ndemand) \tag{14}$$

2.5.4. N balance in the plant

As for the biomass, the N flux at the grassland scale is the combination of the flux in each of the compartments: *NQGV*, *NQGR* (kg N ha^{-1}), the N content of the green compartments (Eq. (17), (18)), and *NQDV*, *NQDR* (kg N ha^{-1}), the N content of the dead compartments (Eq. (15), (16)). The daily variation of the plant N content corresponds to the difference between the absorbed soil nitrogen (*Nuptake*, kg N ha^{-1}, Eq. (14)) that remains in the above-ground biomass [27] and nitrogen that is lost through senescence (*SEN*, kg DM ha^{-1}) for green compartment or abscission (*ABS*, kg DM ha^{-1}) for dead parts. These variations are described by the following equations:

$$\frac{dNQDV}{dt} = ((1 - \sigma_{GV}) \times SENGV - ABSDV) \times propND \tag{15}$$

$$\frac{dNQDR}{dt} = ((1 - \sigma_{GR}) \times SENGR - ABSDR) \times propND \tag{16}$$

$$\frac{dNQGV}{dt} = \begin{cases} Nuptake \times FNH \times \dfrac{GROGV}{GRO} - SENGV \times propND, if\ GRO > 0 \\ -SENGV \times propND, if\ GRO \leq 0 \end{cases} \tag{17}$$

$$\frac{dNQGR}{dt} = \begin{cases} Nuptake \times FNH \times \dfrac{GROGR}{GRO} - SENGR \times propND, if\ GRO > 0 \\ -SENGR \times propND, if\ GRO \leq 0 \end{cases} \tag{18}$$

where σ_{GV} and σ_{GV} denote the rates of biomass loss by respiration during senescence for the GV and GR compartments, respectively (Table B1). The daily variation of *SEN* and *ABS* is detailed in appendix A (Eqs. (A.23), (A.24)). *propND* is the N content in the dead material that goes to the soil by abscission. It is fixed at 8 g N kg^{-1} DM [20]. The fraction of absorbed N (FNH) that remains in the aboveground biomass increases when the N status of the plant increases following a formalism proposed in CATIMO. It varies with the PFT (Eq. (A.39)).

2.5.5. N balance in the soil

N dynamics in Gras-Sim is essentially based on CATIMO and MoSt GG models. Soil N is divided into two pools, organic (*Norg*, kg N ha^{-1}) and mineral N (*Nmin*, kg N ha^{-1}). In case of a mineral N supply (*Nminfertilizer*, kg N ha^{-1}), the whole supply is added to the mineral pool. When organic fertilizer is applied (*Norgfertilizer*, kgN ha^{-1}) the amount of nitrogen added to the mineral pool will depend on the percentage of mineral N (*PropNmin*) in the fertilizer (Eq. (20)). The mineralization process (*mineralization*) reduces N in the organic pool (Eq. (19)) and increases N in the mineral pool, while immobilization (*immobilization*) reduces N in the mineral pool and increases N in the organic pool. The immobilization and mineralization equations are presented in appendix A (Eqs. (A.50), (A.51)). Although less important, some N is brought by rain events (*Nfromrain*, kg N ha^{-1}) to the mineral pool, which can lose N through leaching (*NLeached*, kg N ha^{-1}). The potential N supply from symbiotic legume fixation (*Nfromlegume*) is included in the N balance, although it is not currently modeled. The global N balance in the soil is given by the following equations:

$$\frac{dNorg}{dt} = immobilization + (1 - PropNmin) \times Norgfertilizer + Nplantlitter - mineralization \tag{19}$$

#

$$\frac{dNmin}{dt} = mineralization + PropNmin \times (1 - NH3volatfactor) \times Norgfertilizer + Nfromrain + Nminfertilizer + Nfromlegume - immobilization - Nuptake - NLeached \quad (20)$$

#

where *Nplantlitter* (kg N ha^{-1}) denotes to the total amount of N that goes from the plant to the soil through the dead material (Eq. (A.47)). *NH3volatfactor* is a special factor that allows to consider the amount of N that is lost by volatilization during the fertilizer application (Eq. (A.46)). The formalisms of *NLeached* and *Nfromrain* are also given in appendix A (Eqs. (A.48), (A.49)). The *Nfromlegume* value is zero.

2.6. Management options

As Gras-Sim is under its present form designed for ungrazed grasslands, the management levers are limited to fertilization and cutting. The management strategy will be different according to the functional group and the objectives of simulation. The sward height is the key factor that allows to calculate the biomass available before and after cutting as well as the exported quantity. The N supplied at different periods in mineral or organic form is allocated to the two soil N pools in the proportions described above.

2.7. Model evaluation

2.7.1. Data base for model evaluation

The data used for the model evaluation originated from varietal trials conducted on three sites across Wallonia by Fourrages Mieux (Marche-en-Famenne, Belgium) from 2010 to 2018: Michamps (MCP, 50°03′N 5°80′E), Louvain-la-Neuve (LLN, 50°67′N 4°64′E), and Tinlot (TLT, 50°50′N 5°39′E). The experiments were conducted under controlled agricultural conditions. The trials were performed on 2 m × 7 m experimental plots. An average of 17 varieties were used per trial and per site, with each variety occupying 4 plots. Several data were collected from these different trials. The data used in this document are the yields for 66 cuts performed during the experimental period (Table 2). The PFT A is represented by perennial ryegrass (*Lolium perenne*) and PFT B by orchard grass (*Dactylis glomerata*). To obtain the biomass yield for a given cut, 4 replications were performed at the same date at different locations on the experimental area. The average of the replications was then used as the yield of the cut. The yields of the 4 replications per cut were not available for all cuts. The cuts for which this data was available are represented on the graphs with error bars.

Each experimental site had its own weather station whose data are collected, managed and made available to the public by the Agriculture, Land, and Technology Integration Unit of the Wollon Agricultural Research Center (CRA-W). This data can be downloaded at different time steps from the Agromet platform [32]. The meteorological data used as input to the model were daily average temperature (T), radiation (Ra), potential evapotranspiration (PET), and rainfall (PP) (Table 3).

Overall, LLN received the least amount of water during the experimental period, 499 mm in 2018, in contrast to MCP which recorded the maximum amount, 1105 mm in 2012. Potential water stress (PP-PET) must have been more pronounced in 2018, which was the least rainy year for all sites (Table 3). Only experiment years were considered for each site.

The field trials were governed by one single protocol followed on all sites. The management data used for the evaluation of the model were: cutting dates, number of cuts, fertilization dates, and type of fertilizer and quantities applied. Three cuts were made on average per season. Fertilizer was applied in mineral form before the first cut. Second application was made after the first cut. The third application was made after the second cut if necessary. The amount of nitrogen in the form of nitrate per application averaged 60 kg N ha^{-1}. Phosphorus and potassium in the form of P_2O_5 and K_2O were applied almost systematically at the beginning of each trial. On average, 100 kg of P_2O_5 and 200 kg of K_2O were applied per hectare per trial.

Soil texture varied from site to site. Each site was characterized by its organic matter (OM), clay, and sand content. These proportions being difficult to obtain for the different sites, they were deduced from the type of soil. The soil map of Wallonia was first consulted on the geoportal website [33], then the texture diagram [34] was used to determine the proportion of each element. Overall, the soils are silty with favorable natural drainage at LLN, silty with moderate natural drainage at TLT, and silty-stony with favorable natural drainage at MCP. The sward height at the end of winter was 5 cm. All cuts were made at 5 cm from the ground and each simulation covers 365 days.

2.7.2. Statistical analyses

Model outputs were compared to field data in order to evaluate the ability of the model to predict biomass production. Three statistical indicators were used: relative root mean square error (RRMSE), normalized deviation (ND), and model efficiency (EF). The RRMSE was obtained by dividing the RMSE by the mean of the observed data. The model is considered good for values of RRMSE $\leq$0.20 [35], ND $<$ 0.10, and EF $>$ 50 [36].

$$RRMSE = \frac{1}{\overline{O}} \times \sqrt{\frac{\sum_{i=1}^{n}(Si - Oi)^2}{n}} \quad (21)$$

$$ND = \frac{\sum_{i=1}^{n} Oi - \sum_{i=1}^{n} Si}{\sum_{i=1}^{n} Oi} \quad (22)$$

$$EF = \frac{\sum_{i=1}^{n}(Oi - \overline{O})^2 - \sum_{i=1}^{n}(Si - Oi)^2}{\sum_{i=1}^{n}(Oi - \overline{O})^2} \quad (23)$$

where $\overline{O}$ denotes the mean of the observations, *Oi* the observed value, and *Si* the simulated value. Since the comparison is done by cut, *i* represents the cut.

The sensitivity analysis of the model focused on the impact of three key parameters on biomass production. These parameters were the crop coefficient (*Kc*) which is used in the calculation of the actual evapotranspiration, the maximum absorbable fraction of available *Nmin* (FNA_{max}) which varies between 0 and 1 [27], and the soil *Nmin* content (0–45 cm) for maximum availability (NS_C) which varies between 50 and 400 kg N ha^{-1} [27]. These last two parameters are used to calculate the actual amount of N that can be taken up by the plant from the soil.

3. Results

3.1. Model predictions by functional type

The behavior of the model according to functional type was evaluated by monitoring the dynamics of biomass, mineral N, soil water, and water stress function over two consecutive years.

3.1.1. Predictions for PFT A

The behavior of the model for PFT A was evaluated through a simulation performed on the Louvain-la-Neuve (LLN) site between 2017 and 2018. Nitrogen was applied in mineral form three times and four cuts were made per season (Fig. 2). The total biomass curve shows that biomass accumulation stoped and restarted with each cut. Mineral N in the soil also responded well to fertilization. Each application of mineral N was added directly to the soil mineral N pool. The water stress function was aligned with the soil water content curve (Fig. 2).

Considering all these curves, biomass production in PFT A was strongly linked to soil water and N dynamics. Spring production was highest, over 5 t DM ha^{-1}, under conditions that were not water or N stressed. As summer progresses, water stress slowed biomass

accumulation despite the availability of soil mineral N, resulting in yields of less than 4 t DM ha^{-1} for the second and third cuts (Fig. 2). The last cut also remained low (below 2 t DM ha^{-1}), this time not due to lack of water but rather to lack of mineral N. Overall, PTF A was highly sensitive to water stress, with third cut yields below 1 t DM ha^{-1} in 2018, when stress was at its peak. Stressed plants therefore absorbed less N, resulting in higher soil mineral N levels at the end of the 2018 season compared to the previous season.

3.1.2. Predictions for PFT B

A simulation performed on the Michamps site (MCP) between 2015 and 2016 was used to evaluate the behavior of the model for PFT B. Nitrogen in mineral form was applied three times, with an average of four cuts per season (Fig. 3). The model responded well to the cuttings and N mineral inputs. The soil water and water stress curves remained aligned.

PFT B was less precocious than PFT A, with lower early season biomass accumulation than PFT A. There was more than a ton difference in dry matter between the simulated first cut yields of these two PFTs. Type B was relatively insensitive to small variations in soil water content, maintaining or increasing its production in Cuts 2 and 3 (Fig. 3). Like PFT A, Type B was sensitive to variations in soil N, with a very low yield in the fourth cut (less than 1.5 t DM ha^{-1}) despite water availability.

3.2. Model predictions against field data

The comparison of the simulated data against the observed data, presented in Table 4, indicate an RRMSE and an overall EF of 29 % and 71 % for biomass. The overall ND was below 10 % for biomass. Organic matter digestibility was not evaluated.

3.2.1. Biomass per cut

The average biomass simulated per cut was close to the field biomass, with a maximum difference of 0.1 t DM ha^{-1} observed at cut 1. Simulated yields per cut were highly correlated with measured yields (Fig. 4). The first cut, the most important of the season, was predicted with a RRMSE of 21 % and a ND lower than 10 %. The yield at cut 2, remained relatively less well predicted compared to cut 1 with an RRMSE slightly higher than 30 % (Table 4). Biomass at cut 3 also was less well predicted compared to the first cut with an RRMSE value above 30 % (Table 4). As with cut 2, the yield at cut 3 was predicted with ND values below 10 % and EF above 60 % (Table 4). The fourth and fifth cuts were less well predicted compared to the first three. However, the smaller number of data available for the latter two cuts could explain the poorer predictions.

3.2.2. Biomass production by PFT

The model predicted the yields of both PFTs with a strong correlation between field and simulation data (Fig. 5). Biomass production of PFT A was predicted with a difference between observed and simulated yields of less than 0.05 t DM ha^{-1}. The low ND, less than 3 %, confirms the predictive quality of the model for each cut of TFP A taken separately. Compared to PFT A, the model predicted PFT B biomass production closer to that of the field, 0.1 t difference (Table 4). The RRMSE was less than 30 % and the ND below 5 % with an EF above 70 %.

3.3. Model response to water and nitrogen stress

3.3.1. Nitrogen stress

The effect of N stress on yield was evaluated in the orchard-grass trial (PFT B) conducted at LLN between 2014 and 2016, where no N application was made. To avoid a combination of the effect of water stress and N stress, the results of 2016 were presented. The year 2016 was one of the three years with a positive average water balance (PP-PET), 3 mm (Table 3).

Nitrogen application reduced the effect of N stress by shifting the N stress function curve above the 0.5 threshold before each cut, whereas it was almost zero before the first cut and practically below 0.5 before the other cuts in unfertilized conditions (Fig. 6). The reduction in nitrogen stress resulted in an increase in biomass production, which reached 5 t in the first cut and 3 t in the second cut (Fig. 6). Biomass production was less than 4 tons in the first cut and 2 tons in the second cut under trial conditions.

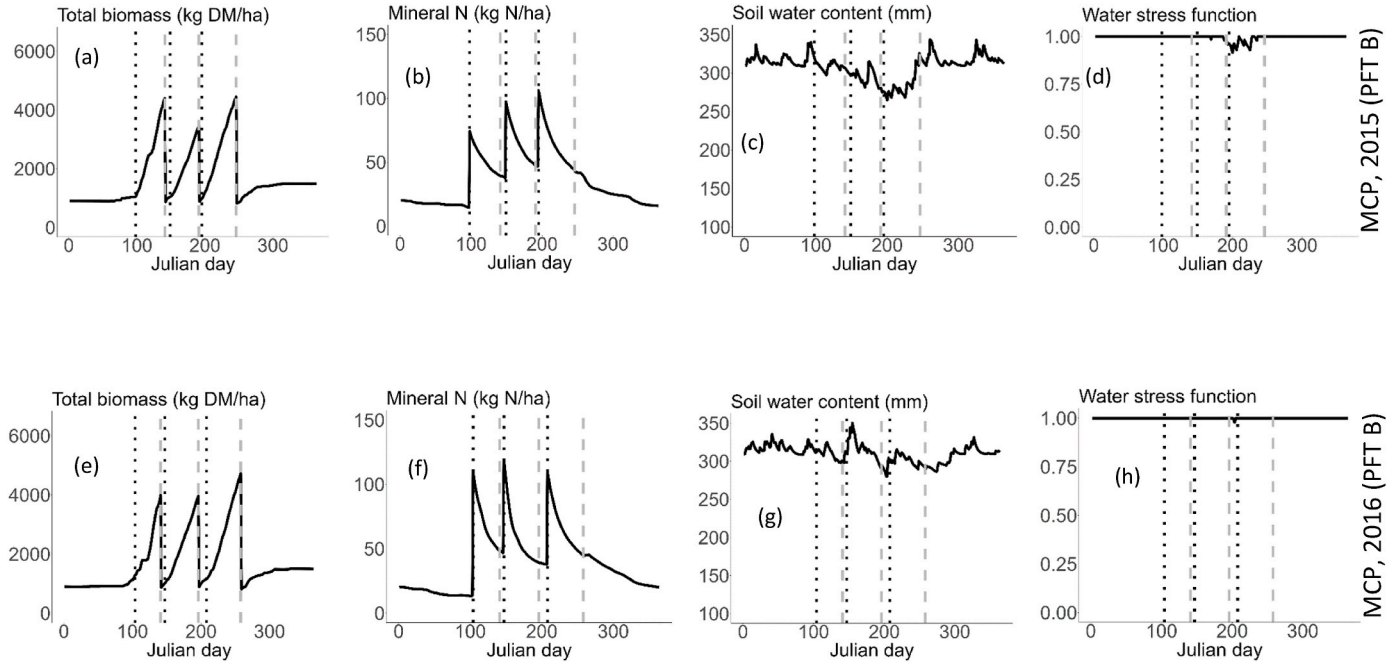

Fig. 3. Dynamics of above-ground biomass, soil water and nitrogen, and water stress function, simulated by Gras-Sim on the Michamps (MCP) site for PFT B over two consecutive years: 2015 ((a), (b), (c), and (d)) and 2016 ((e), (f), (g), and (h)). The grey dashed lines correspond to cutting dates and the black dashed lines correspond to fertilization dates.

Table 4
Comparison between field data and Gras-Sim predicted data for biomass. Mean values are presented with the standard deviation between brackets. C1, C2, C3, C4, and C5 represent the first, second, third, fourth, and fifth cuts, respectively. A and B are PFTs.

Biomass (kg DM ha^{-1})								
	Total (n = 66)	A (n = 27)	B (n = 39)	C1 (n = 21)	C2 (n = 17)	C3 (n = 16)	C4 (n = 10)	C5 (n = 2)
Observed	2643 (1463)	2606 (1341)	2668 (1558)	4006 (1365)	2278 (837)	2078 (1162)	1571 (946)	1303 (884)
Simulated	2600 (1469)	2652 (1310)	2564 (1586)	4124 (975)	2141 (945)	2198 (1267)	1196 (385)	749 (335)
RRMSE	0.29	0.3	0.29	0.21	0.34	0.33	0.5	0.52
ND	0.02	0.02	0.04	0.03	0.06	0.06	0.24	0.43
EF	0.71	0.66	0.74	0.59	0.08	0.64	0.24	−0.17

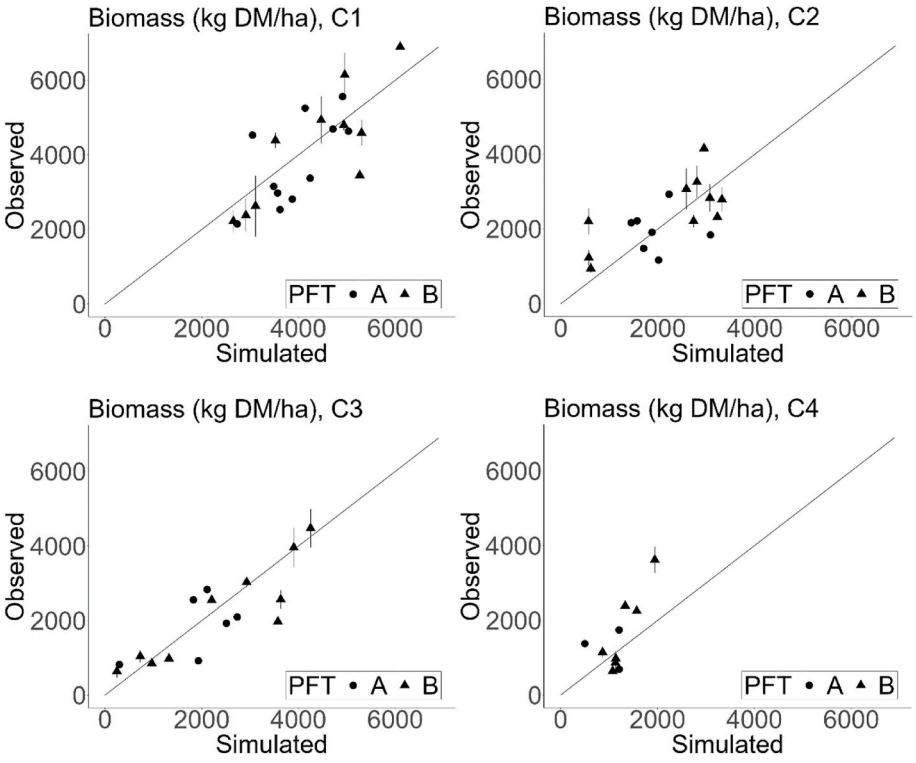

Fig. 4. Comparison of observed and simulated biomass for the first 4 cuts (C1, C2, C3, and C4 represent the first, second, third, and fourth cuts, respectively). The yields per cut for which replication data (4 measurements) are available, are presented with error bars.

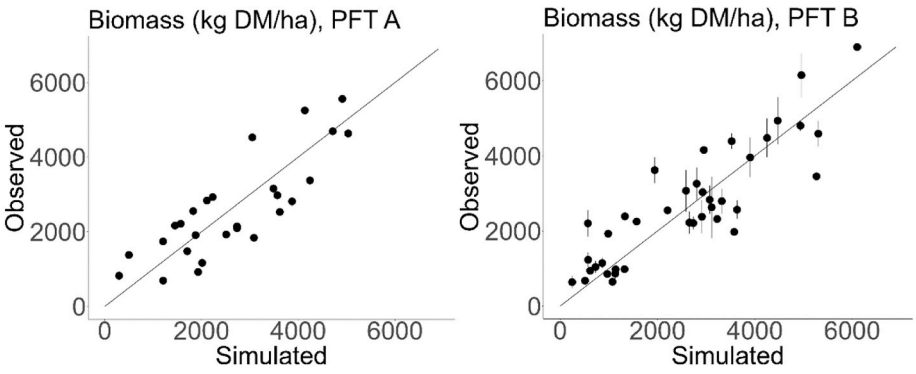

Fig. 5. Comparison of observed and simulated biomass per cut for plant functional types A and B. The yields per cut for which replication data (4 measurements) are available, are presented with error bars.

3.3.2. *Water stress*

The response of the model to water stress was evaluated by considering four contrasting conditions in terms of water balance (PP-PET). The year 2012, which recorded the largest water excess of 683 mm on the MCP site (Table 3), was the one in which the curve of the water stress function remained strictly equal to 1, reflecting an absence of stress (Fig. 7).

Conversely, 2018, which recorded a water deficit of 316 mm on the LLN site (Table 3), showed a water stress curve almost below the threshold of 0.5 between the second and third cuts. The water stress

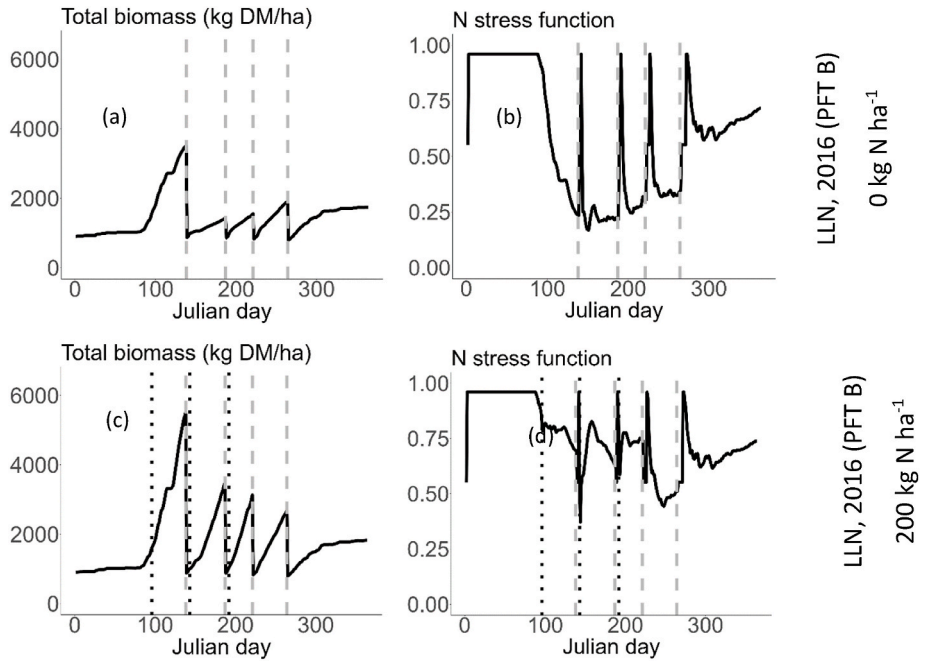

Fig. 6. Dynamics of aboveground biomass and N stress function, simulated by Gras-Sim for PFT B on the Louvain-la-Neuve (LLN) site in 2016 with 0 kg N ha-1 ((a) and (b)) and 200 kg N ha-1 ((c) and (d)). The grey dashed lines correspond to cutting dates and the black dashed lines correspond to fertilization dates.

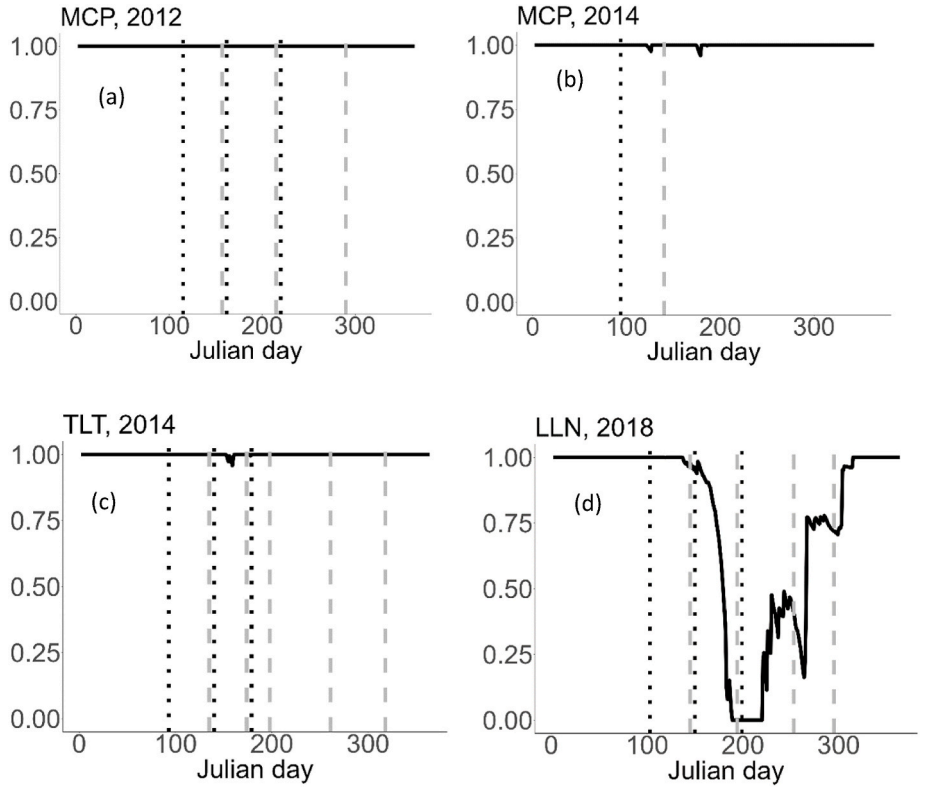

Fig. 7. Dynamics of the water stress function, simulated by Gras-Sim at Michamps (MCP) in 2012 with a water balance (PP-PET) of 683 mm (a) and 2014 with a (PP-PET) of 175 mm (b), Tinlot (TLT) in 2014 with a (PP-PET) of 147 mm (c) and Louvain-la-Neuve (LLN) in 2018 with a negative (PP-PET), - 316 mm (d). The dashed lines correspond to the cutting dates.

curve in 2014 at the MCP and TLT sites remained above the 0.95 threshold (Fig. 7). The year 2014 was less wet than 2012, but much wetter than 2018, with an average surplus of 160 mm (Table 3).

3.4. Sensitivity analysis of the model

The effect of the crop coefficient (Kc), the maximum absorbable fraction of available Nmin (FNA_{max}), and the soil Nmin content (0–45 cm) for maximum availability (NS_C) on the biomass production was

Table 5
Sensitivity analysis of biomass production for Kc, FNAmax, and NSc parameters. Values are model outputs in response to different variations of Kc, FNAmax, and NSc parameters. C1, C2, C3, C4, and C5 represent the first, second, third, fourth, and fifth cuts, respectively. A and B are PFTs. Mean values are presented with the standard deviation between brackets.

	Kc				FNAmax				NSc			
	−0.2	−0.1	+0.1	+0.2	−0.02	−0.01	+0.01	+0.02	−20	−10	+10	+20
Biomass (kg DM ha^{-1})												
Total	2598 (1427)	2622 (1444)	2509 (1503)	2364 (1589)	2583 (1459)	2592 (1464)	2608 (1474)	2616 (1479)	2648 (1498)	2624 (1484)	2577 (1456)	2555 (1442)
A	2746 (1250)	2738 (1279)	2541 (1407)	2421 (1535)	2635 (1302)	2644 (1306)	2661 (1314)	2669 (1318)	2702 (1334)	2677 (1322)	2629 (1299)	2606 (1288)
B	2496 (1545)	2542 (1559)	2487 (1583)	2325 (1644)	2548 (1575)	2556 (1580)	2572 (1591)	2580 (1597)	2610 (1618)	2587 (1602)	2542 (1571)	2520 (1556)
C1	4074 (967)	4101 (972)	4143 (977)	4160 (976)	4094 (970)	4109 (973)	4138 (978)	4152 (980)	4206 (989)	4164 (982)	4084 (968)	4046 (961)
C2	2143 (979)	2176 (975)	2032 (981)	1789 (1059)	2125 (941)	2133 (943)	2148 (947)	2156 (949)	2185 (957)	2162 (951)	2119 (939)	2099 (933)
C3	2313 (1069)	2285 (1182)	1930 (1174)	1582 (1159)	2186 (1261)	2192 (1264)	2204 (1270)	2210 (1273)	2233 (1285)	2216 (1276)	2182 (1259)	2166 (1251)
C4	1110 (347)	1193 (413)	1158 (480)	1122 (644)	1193 (385)	1194 (385)	1198 (386)	1199 (386)	1205 (386)	1200 (385)	1192 (384)	1187 (384)
C5	691 (295)	719 (315)	791 (369)	865 (440)	747 (333)	748 (334)	750 (336)	751 (337)	756 (341)	752 (338)	746 (333)	743 (330)

tested throughout the experimental period for the 5 cuts and 2 PFTs (Table 5). The initial value of Kc was decreased and increased by 0.1 and 0.2. FNA_{max} was decreased and increased by 0.01 and 0.02. NS_C was increased and decreased by 10 and 20 kg N ha^{-1}. These different values were chosen according to the order of magnitude of the parameters, as has been the case in other works [22,36]. The aim was to have a more or less significant change in the outputs, in order to better assess the sensitivity of the model to these parameters.

A decrease in FNA_{max} consistently resulted in a decrease in yield for all PFTs and cuts. Similarly, as FNA_{max} increased, the simulated yield increased. An increase of 0.02 in FNA_{max} increased the total yield by 5 % and the yield of PFTs A and B by 6 % and 5 %, respectively. A decrease of 0.02 in FNA_{max} decreased the yield by 8 % for both total production and that of PFT A and B. Decreasing the Kc value led to an overall increase in biomass production. A decrease in Kc of 0.1 increased total production by 1 %. The total biomass produced tended to decrease at higher Kc values. An increase in Kc of 0.1 resulted in a 4 % decrease in biomass from baseline production and an increase of 0.2 resulted in a 9 % loss in production. PFT A was most sensitive to low Kc values. A decrease in Kc of 0.2 resulted in a 3 % increase in yield. An increase in the value of Kc of 0.1 resulted in a 4 % decrease in yield for PFT A and 3 % decrease for PFT B. Increasing Kc by 0.2 resulted in a loss of biomass of 9 % for both PFTs A and B. The yield was sensitive to increases in Kc for all cuts. Biomass loss varied between 0 and 28 % for all cuts when Kc was increased by 0.2.

The yield increased systematically as the value of the parameter NS_C was decreased for all PFTs and regardless of the cut. Conversely, the higher the NS_C value, the lower the yield. A decrease in the value of NS_C by 20 kg N ha^{-1} increased total production by 2 % and a decrease in its value by 10 kg N ha^{-1} increased total production by 1 %. Conversely, an increase in NS_C of 10 kg N ha^{-1} decreased total yield by 1 %, while an increase in NS_C of 20 kg N ha^{-1} decreased total yield by 2 %. The sensitivity of yield to NS_C variation was almost the same for both PFTs. Decreasing NS_C by 20 kg N ha^{-1} resulted in a 3 % increase in yield for both PFTs, while decreasing NS_C by 10 kg N ha^{-1} resulted in a 1–2 % increase in yield. Increasing NS_C by 20 kg N ha^{-1} resulted in 3 % loss of biomass for both PFT A and B. The first two cuts were more sensitive to changes in NS_C. The gain in biomass for these two cuts was 2 % when the NS_C value was decreased by 20 kg N ha^{-1}, compared to an increase of 1 % for the last three cuts. Similarly, a 20 kg N ha^{-1} increase in NS_C resulted in a 2 % decrease in yield for the first two cuts versus a 1 % loss for the last three cuts over the experimental period.

4. Discussion

This first evaluation of the Gras-Sim model showed that the simulation results were quite close to the field data. The model had a good response to water and nitrogen stress. It was evaluated on data collected on 3 different sites in Wallonia with different pedoclimatic characteristics and over several years.

4.1. Features of the Gras-Sim model

Compared to ModVege, Gras-Sim does not only describe soil water dynamics, but also nitrogen dynamics. This was partially the case in MoSt GG model. However, the formalism on the dynamics of nitrogen in the soil and in the plant presented in Gras-Sim is based on the nitrogen dilution curves which can be parameterized according to the plant functional type. The equations of daily N demand and N uptake are different from those of Ruelle et al. [20]. They are based on the formulas proposed in CATIMO model [27]. Since the aboveground biomass is divided into four compartments, representative of the structural components of the grass, as presented in ModVege, Gras-Sim allows to simulate separately the N content of the dead and green compartments. Gras-Sim also proposes a new approach to convert potential evapotranspiration into actual evapotranspiration. This rather original approach is based on the specific crop coefficient (Kc) for grasslands and for a given geographical area.

4.2. Simulation results: total biomass production

The seasonal dynamics of PFT A and B plants were well described by the model. PFT B plants are fertile environmental species, but less precocious than PFT A plants. This resulted in early season yields generally lower than those of PFT A (Figs. 2 and 3). This is in agreement with the characteristics of the different PFTs described by Cruz et al. [10].

The lack of data for the fourth and especially the fifth cut would explain why the yield for these cuts was less well predicted by the model. In fact, for these two cuts, the RRMSE was higher than 35 % and the ND higher than 10 % [36]. A practicality of Gras-Sim, compared to other models such as MoSt GG [20], is its ability to simulate the daily dynamics of several grass species distributed in plant functional types (PTFs) A and B. The parameterization of these different PFTs is based on that of Jouven et al. [22], revised on the basis of the new classification of functional types presented by Cruz et al. [10]. The ND values well below 10 % and EF values above 60 % reflect the predictive quality of the above ground biomass of the two PFTs [36]. The idea in the design of

Gras-Sim was to have a model with fewer parameters and input data on soil nitrogen at the beginning of the simulation, easily measurable in the field. The effect of the simplified soil nitrogen dynamics formalism on the yield was reflected in the sensitivity of the model to the parameter FNA_{max}, which is used in the calculation of the fraction of soil N available to the plant. The model was sensitive even to small variations in FNA_{max}, which would explain why in MoSt GG model, the minimum value of FNA (FNA_{min}) was set at 0.00012 and that of FNA_{max} at 0.00014 [20], a difference of 0.00002 between the minimum and maximum value.

4.3. Biomass and AET formalism

Using the crop coefficient (Kc) adapted for grassland in estimating the AET from the PET is a major step forward in grass growth modeling. Monthly average Kc values can be obtained for a large part of the European countries participating in the FLUXNET network. The use of Kc for grassland allows to consider the local soil and climate conditions, which can vary widely from one region to another. The new AET formalism would limit the tendency of ModVege to overestimate the impact of moderate water stress on growth and consequently on biomass production [26]. Using Kc finally allows to have a common formalism for both crops and grasslands. Biomass production was sensitive to the value of Kc parameter with variability between PFT and number of cuts. PFT A plants, due to their characteristics [10], are able to better utilize the soil water reserve to produce more biomass, which is not necessarily the case for PFT B plants, since water stress is not the only growth limiting factor. Reducing the Kc value by 0.1 increaseed the yield by 3 % for PFT A. The higher the Kc values, the more the plants are exposed to the risk of heat stress and the less they will produce. This is in agreement with the work of Stratigea and Makropoulos [37] who showed that as Kc increases, the water demand of the plants increases. This resulted in a biomass loss of 9 % for both PFT A and PFT B when the Kc was increased by 20 %.

4.4. Validity fields of the Gras-Sim model

Gras-Sim, like the previous ModVege [22] and MoSt GG [20] models, was designed for grass-dominated grasslands. As parameterized, Gras-sim can simulate the dynamics of grasslands dominated by plants of functional type A (e.g.*Lolium perenne*) and type B (e.g. *Dactylis glomerata*) as classified by Cruz et al. [10]. The model parameters can be divided into two blocks: those related to biomass dynamics and those related to soil and plant N dynamics. Biomass parameters were calibrated on the basis of Cruz et al. [10] values for parameters with little environmental influence, such as average leaf lifespan and specific leaf area, or on the basis of field data and simulations performed over several years at the three study sites in Wallonia (Belgium). N parameter values were also taken from field data and simulations or the literature, in particular for the N dilution curves [30,31]. Gras-Sim is therefore a model that can be used to predict biomass production in grass-dominated grasslands throughout Wallonia. Based on climate forecasts, Gras-Sim can be used in research to predict the impact of different management strategies (cutting dates, fertilization dates, fertilizer quantities, etc.) on the resistance and resilience of permanent grasslands in the face of climate change. On a technical level, Gras-Sim can be used as a starting point for the design of a decision support tool for livestock farmers.

4.5. Further work

After this first confirmation of Gras-Sim simulation results with field data, the next step will be to confront the model with other pedoclimatic conditions using a large database covering several years with a significant number of cuts, as Beaudoin et al. [36] did for the STICS model.

Gras-Sim currently simulates the daily dynamics of biomass production for PFTs A and B. It would be interesting in a future development to extend the model to PFTs C and D as it is the case in ModVege. The model should then be extended to legumes and other PFTs as presented in DynaGraM [25], with an evolution in time of the proportions of different PFTs based on the availability and access to the resource.

To allow Gras-Sim to simulate the dynamics of grazed grasslands, an animal sub-model will be integrated into the spatialized version of the model. Considering the effects of animal dejections on the soil N pool, as Ruelle et al. [20], and other disturbances associated with animal presence such as trampling. The model will then become more complex and capable of predicting primary and secondary production at the farm level.

5. Conclusion

Gras-Sim is a simple model that can be used as a starting point for building a decision support tool. It allows prediction on the aboveground biomass production based on weather conditions, soil water and nitrogen dynamics. The practicality of Gras-Sim is that it can be used for a large number of grassland species grouped in two PFTs A and B. The AET formalism in Gras-Sim, based on the crop coefficient (Kc) adapted for grassland, allows the prediction of the biomass production even in the period of water stress. This first evaluation in the context of the Walloon region (Belgium) showed that the model responds well to water and nitrogen stress. Future work is needed to validate the model under other soil and climate conditions and to extend it to the whole farm scale.

Declaration of competing interest

The authors declare that they have no known competing financial interests or personal relationships that could have appeared to influence the work reported in this paper.

Data availability

Data will be made available on request.

Acknowledgements

The authors gratefully acknowledge Dr. Ge Sun for the data on crop coefficient (Kc) for grassland and Prof. Magali Jouven for her constructive comments on an earlier version of the manuscript.

Appendix A. Supplementary data

Supplementary data to this article can be found online at https://doi.org/10.1016/j.jafr.2023.100875.

References

[1] P. Dillon, J. Roche, L. Shalloo, B. Horan, Optimising Financial Return from Grazing in Temperate Pastures, Wageningen Academic Publishers, 2005, pp. 131–147, https://doi.org/10.3920/978-90-8686-554-3.
[2] M. O'Donovan, E. Lewis, P. O'Kiely, Requirements of future grass-based ruminant production systems in Ireland, Ir. J. Agric. Food Res. 50 (2011) 1–21.
[3] P.K. Thornton, Livestock production: recent trends, future prospects, Philos. Trans. R. Soc. B Biol. Sci. 365 (2010) 2853–2867, https://doi.org/10.1098/rstb.2010.0134.
[4] F. Piseddu, G. Bellocchi, C. Picon-Cochard, Mowing and warming effects on grassland species richness and harvested biomass: meta-analyses, Agron. Sustain. Dev. 41 (2021) 74, https://doi.org/10.1007/s13593-021-00722-y.
[5] W. Han, L. Chen, X. Su, D. Liu, T. Jin, S. Shi, T. Li, G. Liu, Effects of soil physicochemical properties on plant species diversity along an Elevation Gradient over alpine grassland on the Qinghai-Tibetan plateau, China, Front. Plant Sci. 13 (2022), 822268, https://doi.org/10.3389/fpls.2022.822268.
[6] W. Li, X. Gan, Y. Jiang, F. Cao, X.-T. Lü, T. Ceulemans, C. Zhao, Nitrogen effects on grassland biomass production and biodiversity are stronger than those of phosphorus, Environ. Pollut. 309 (2022), 119720, https://doi.org/10.1016/j.envpol.2022.119720.

[7] P. Cruz, M. Duru, O. Therond, J.P. Theau, C. Ducourtieux, C. Jouany, R.A. H. Khaled, P. Ansquer, Une nouvelle approche pour caractériser les prairies naturelles et leur valeur d'usage, Fourrages (Frankfort On The Main) (2002) 335.
[8] S. Díaz, A. Purvis, J.H.C. Cornelissen, G.M. Mace, M.J. Donoghue, R.M. Ewers, P. Jordano, W.D. Pearse, Functional traits, the phylogeny of function, and ecosystem service vulnerability, Ecol. Evol. 3 (2013) 2958–2975, https://doi.org/10.1002/ece3.601.
[9] P. Cruz, F.L.F. De Quadros, J.P. Theau, A. Frizzo, C. Jouany, M. Duru, P.C. F. Carvalho, Leaf traits as functional descriptors of the intensity of continuous grazing in native grasslands in the South of Brazil, Rangel. Ecol. Manag. 63 (2010) 350–358, https://doi.org/10.2111/08-016.1.
[10] P. Cruz, J.P.J.P. Theau, E. Lecloux, C. Jouany, M.M. Duru, Typologie fonctionnelle de graminées fourragères pérennes : une classification multitraits, Fourrages (Frankfort On The Main) (2010) 11.
[11] A.-I. Graux, Modélisation des impacts du changement climatique sur les écosystèmes prairiaux. Voies d'adaptation des systèmes fourrragers, PhD thesis, Université Blaise Pascal - Clermont-Ferrand II, 2011. https://theses.hal.science/tel-00653360. (Accessed 18 September 2023).
[12] K. Petersen, D. Kraus, P. Calanca, M.A. Semenov, K. Butterbach-Bahl, R. Kiese, Dynamic simulation of management events for assessing impacts of climate change on pre-alpine grassland productivity, Eur. J. Agron. 128 (2021), 126306, https://doi.org/10.1016/j.eja.2021.126306.
[13] N.J.B. Puche, M.U.F. Kirschbaum, N. Viovy, A. Chabbi, Potential impacts of climate change on the productivity and soil carbon stocks of managed grasslands, PLoS One 18 (2023), e0283370, https://doi.org/10.1371/journal.pone.0283370.
[14] M. Filipiak, D. Gabriel, K. Kuka, Simulation-based assessment of the soil organic carbon sequestration in grasslands in relation to management and climate change scenarios, Heliyon 9 (2023), e17287, https://doi.org/10.1016/j.heliyon.2023.e17287.
[15] A.H.C.M. Schapendonk, W. Stol, D.W.G. van Kraalingen, B.A.M. Bouman, LINGRA, a sink/source model to simulate grassland productivity in Europe, Eur. J. Agron. 9 (1998) 87–100, https://doi.org/10.1016/S1161-0301(98)00027-6.
[16] A. Swieter, S. Moenickes, B. Ohnmacht, J.-M. Greef, U. Feuerstein, Monitoring, analysis and modeling of yield and quality dynamics of Lolium perenne varieties for biogas production, in: D. Sokolović, C. Huyghe, J. Radović (Eds.), Quant. Traits Breed. Multifunct. Grassl. Turf, Springer Netherlands, Dordrecht, 2014, pp. 325–330, https://doi.org/10.1007/978-94-017-9044-4_44.
[17] I. Calvache, O. Balocchi, R. Arias, M. Alonso, The use of thermal time to describe and predict the growth and nutritive value of Lolium perenne L. And bromus valdivianus, Phil, Agronomy. 11 (2021) 774, https://doi.org/10.3390/agronomy11040774.
[18] N.J. Hutchings, I.J. Gordon, A dynamic model of herbivore–plant interactions on grasslands, Ecol. Model. 136 (2001) 209–222, https://doi.org/10.1016/S0304-3800(00)00426-9.
[19] D.G. McCall, G.J. Bishop-Hurley, A pasture growth model for use in a whole-farm dairy production model, Agric. Syst. 76 (2003) 1183–1205, https://doi.org/10.1016/S0308-521X(02)00104-X.
[20] E. Ruelle, D. Hennessy, L. Delaby, Development of the Moorepark St Gilles grass growth model (MoSt GG model): a predictive model for grass growth for pasture based systems, Eur. J. Agron. 99 (2018) 80–91, https://doi.org/10.1016/j.eja.2018.06.010.
[21] S.J.R. Woodward, M. Van Oijen, W.M. Griffiths, P.C. Beukes, D.F. Chapman, Identifying causes of low persistence of perennial ryegrass (Lolium perenne) dairy pasture using the Basic Grassland model (BASGRA), Grass Forage Sci. 75 (2020) 45–63, https://doi.org/10.1111/gfs.12464.
[22] M. Jouven, P. Carrere, R. Baumont, Model predicting dynamics of biomass, structure and digestibility of herbage in managed permanent pastures. 1. Model description, Grass Forage Sci. 61 (2006) 112–124, https://doi.org/10.1111/j.1365-2494.2006.00515.x.
[23] F. Piseddu, R. Martin, E. Movedi, F. Louault, R. Confalonieri, G. Bellocchi, Simulation of multi-species plant communities in perturbed and nutrient-limited grasslands: development of the growth model ModVege, Agronomy 12 (2022) 2468, https://doi.org/10.3390/agronomy12102468.
[24] T. Moulin, A. Perasso, F. Gillet, Modelling vegetation dynamics in managed grasslands: responses to drivers depend on species richness, Ecol. Model. 374 (2018) 22–36, https://doi.org/10.1016/j.ecolmodel.2018.02.013.
[25] T. Moulin, A. Perasso, P. Calanca, F. Gillet, DynaGraM: a process-based model to simulate multi-species plant community dynamics in managed grasslands, Ecol. Model. 439 (2021), 109345, https://doi.org/10.1016/j.ecolmodel.2020.109345.
[26] P. Calanca, C. Deléglise, R. Martin, P. Carrère, E. Mosimann, Testing the ability of a simple grassland model to simulate the seasonal effects of drought on herbage growth, Field Crops Res. 187 (2016) 12–23, https://doi.org/10.1016/j.fcr.2015.12.008.
[27] H. Bonesmo, G. Bélanger, Timothy yield and nutritive value by the CATIMO model: I. Growth and nitrogen, Agron. J. 94 (2002) 337–345, https://doi.org/10.2134/agronj2002.3370.
[28] C. Liu, G. Sun, S.G. McNulty, A. Noormets, F. Yuan, Environmental controls on seasonal ecosystem evapotranspiration/potential evapotranspiration ratio as determined by the global eddy flux measurements, Hydrol. Earth Syst. Sci. 21 (2017) 311–322, https://doi.org/10.5194/hess-21-311-2017.
[29] G. Lemaire, J. Salette, M. Sigogne, J.-P. Terrasson, Relation entre dynamique de croissance et dynamique de prélèvement d'azote pour un peuplement de graminées fourragères. I.–Etude de l'effet du milieu, Agronomie 4 (1984) 423–430, https://doi.org/10.1051/agro:19840503.
[30] G. Lemaire, A. Denoix, Croissance estivale en matière sèche de peuplements de fétuque élevée (Festuca arundinacea Schreb.) et de dactyle (Dactylis glomerata L.) dans l'Ouest de la France. I. Etude en conditions de nutrition azotée et d'alimentation hydrique non limitantes, Agronomie 7 (1987) 373–380, https://doi.org/10.1051/agro:19870602.
[31] M.A. Marino, A. Mazzanti, S.G. Assuero, F. Gastal, H.E. Echeverría, F. Andrade, Nitrogen dilution curves and nitrogen use efficiency during winter–Spring growth of annual ryegrass, Agron. J. 96 (2004) 1, https://doi.org/10.2134/agronj2004.0601.
[32] CRA-W/Agromet, Réseau Pameseb, (n.d.). https://agromet.be/en/reseau-pameseb/(accessed September 8, 2021)..
[33] Géoportail Wallonie, Carte des sols de Wallonie, (n.d.). http://geoapps.wallonie.be/Cigale/Public/#CTX=CNSW#BBOX=−43265.277796961105.466058.6575175624.-9775.717478795585.267045.1486629367 (accessed December 15, 2021).
[34] B.B. Bah, P. Engels, G. Colinet, L. Bock, C. Bracke, P. Veron, Légende de la Carte Numérique des Sols de Wallonie (Belgique). Sur base de la légende originale de la Carte des sols de la Belgique de l'IRSIA à 1/20.000, 2005.
[35] M. Despotovic, V. Nedic, D. Despotovic, S. Cvetanovic, Evaluation of empirical models for predicting monthly mean horizontal diffuse solar radiation, Renew. Sustain. Energy Rev. 56 (2016) 246–260, https://doi.org/10.1016/j.rser.2015.11.058.
[36] N. Beaudoin, M. Launay, E. Sauboua, G. Ponsardin, B. Mary, Evaluation of the soil crop model STICS over 8 years against the "on farm" database of Bruyères catchment, Eur. J. Agron. 29 (2008) 46–57, https://doi.org/10.1016/j.eja.2008.03.001.
[37] D. Stratigea, C. Makropoulos, Balancing water demand reduction and rainfall runoff minimisation: modelling green roofs, rainwater harvesting and greywater reuse systems, Water Supply 15 (2015) 248–255, https://doi.org/10.2166/ws.2014.105.